7th AIAA/CEAS Aeroacoustics Conference
28-30 May 2001 Maastricht, Netherlands

A01-30853

AIAA-2001-2196

AERODYNAMIC NOISE PREDICTION USING PARALLEL METHODS ON UNSTRUCTURED GRIDS

Lyle N. Long*, Frederic Souliez† and Anupam Sharma†
Department of Aerospace Engineering
The Pennsylvania State University, PA-16802

Aerodynamic noise from a cone in a uniform flow is computed using the Ffowcs Williams-Hawkings (FW-H) equation. The time accurate flow data is obtained using a finite volume flow solver on an unstructured grid. The FW-H equation is solved for surface integrals over a permeable surface away from the cone. Predictions from the FW-H code are compared with direct calculations by the flow solver at a few observer locations inside the computational domain. A very good qualitative match is obtained. Sound directivity patterns in the azimuthal and in the longitudinal directions are presented. The FW-H code is also validated against a model problem of a monopole in a uniform mean flow.

Nomenclature

C_p	coefficient of pressure
C_s	sub-grid scale constant in Smagorinsky model
c	sound speed in quiescent medium
d	base diameter of the cone
f_s	vortex shedding frequency (Hz)
$H(f)$	Heaviside function, $H(f) = 0$ for $f < 0$ and $H(f) = 1$ for $f > 0$
L_i	refer Eq. 2
L_M	$L_i M_i$
L_r	$L_i \hat{r}_i$
$\dot{L}_r$	$\dot{L}_r \hat{r}_i$
$\mathbf{M}$	local Mach number vector of the source
M	$\lvert\mathbf{M}\rvert$
M_n	$M_i \hat{n}_i$
M_0	U_0/c
M_r	$M_i \hat{r}_i$
$\dot{M}_r$	$\dot{M}_i \hat{r}_i$
$\hat{\mathbf{n}}$	unit normal vector to the surface, n_i
P_{ij}	compressive stress tensor with $p_o \delta_{ij}$ subtracted
p	pressure
p_0	freestream pressure
p'	acoustic pressure, $p - p_o$
p'$_{rms}$	root mean squared pressure perturbation
ret	retarted time
T_{ij}	Lighthill stress tensor
t	observer time
θ	angular location of the observer
U	averaged streamwise velocity
U_0, U_∞	freestream velocity
U_i	refer Eq. 2
U_n	$U_i \hat{n}_i$
$\dot{U}_n$	$\dot{U}_i \hat{n}_i$
$U_{\dot{n}}$	$U_i \dot{\hat{n}}_i$
u_i	components of local fluid velocity
u'_{avg}	averaged streamwise perturbation velocity
u_n	$u_i \hat{n}_i$
v_n	local normal velocity of the source surface
$\delta(f)$	Dirac delta function $\delta(f) = 1$ for $f = 0$, otherwise $\delta(f) = 0$
δ_{ij}	Kronecker delta function, $\delta_{ij} = 1$ for $i = j$, otherwise $\delta_{ij} = 0$
ρ	density of the fluid
ρ_0	freestream density of the fluid
ρ'	density perturbation, $\rho - \rho_o$
Ω	vorticity (s^{-1})
ω	angular frequency of the monopole source
$\Box^2$	wave operator, $\Box^2 \sim (\frac{1}{c^2}\frac{\partial^2}{\partial t^2} - \nabla^2)$

Introduction

RECENTLY, the Ffowcs Williams-Hawkings (FW-H) equation has been used with permeable surfaces for predicting aerodynamic noise. The application of FW-H in this manner effectively allows for the inclusion of the quadrupole source terms inside the surface without performing volume integrations. This has significantly improved the accuracy of noise prediction for cases where the contribution from nonlinear interactions in the flow cannot be ignored. This is typical of highly turbulent flows, for example, high Reynolds number jets and wakes.

The FW-H equation requires time accurate data on, and in the volume inside the permeable surface. This data is usually obtained by solving the Euler/Navier-Stokes equations accurately in time. Since the FW-H equation uses data from within the FW-H surface, the

*Professor, Assoc. Fellow, AIAA. lnl@psu.edu.
†Graduate Research Assistant, Pennsylvania State University

outer grid can be made coarse without much loss of accuracy. Unstructured grids provide great flexibility in distributing the grid in the domain, and hence can be used to cluster the cells inside the FW-H surface. This feature can be exploited to significantly increase the computation speed while keeping almost the same accuracy in predicting aerodynamic noise. This will also permit the modeling of complex geometries such as helicopter fuselages, landing gear, and flaps.

The goal here is to test the combination of unstructured grids with the FW-H equation in predicting the aerodynamic noise. The test case is chosen to be the flow over a cone. A cone has sharp edges which fixes the separation point. This makes the flow fairly Reynold's number independent.

We use the Parallel Unstructured Maritime Aerodynamics (PUMA)[1] code for generating the time-accurate flow data. PUMA has been validated for time-accurate computations.[2–4] The ultimate aim is to predict the airframe noise from complex geometries such as landing gear, slats, and flaps. This cone case may be considered as a benchmark problem.

The Grid

The grid used for the simulation of the flow over a cone of vertex angle 60° was generated using Gridgen. Figure 1 shows an overall view of the mesh consisting of approximately 280,000 tetrahedra. The clustering was done around the cone and in the wake region with increasing cell size towards the outer boundaries of the computational domain. The reason for using Gridgen comes from one interesting feature of this commercial software: arbitrary surfaces can be created around the cone (one within the CFD domain boundaries and the other being the CFD domain boundary) and are sources for the meshing algorithm. It is possible to export separately any of these closed surfaces in a separate file, providing a means to extract flow data on the surface using a FW-H module that was added to the unstructured solver. The smallest cylinder was used as a porous FW-H surface. At the bounding faces of the CFD domain, Riemann boundary conditions were assigned at each face center, hence minimizing reflections from the boundaries into the computational domain. The large cells in the far-field also help dissipate any reflections. A no-slip condition was used at the solid surface, even though the boundary layer was not resolved due to computer limitations.

By using a set of faces that are actually used by the flow solver during the computation, there is no additional work required to extract the data needed for the far-field noise. This type of FW-H surface also reflects the true mesh clustering present where the flow variables are locally being computed: there is no loss in accuracy due to the interpolation onto a surface whose refinement might not be that of the computational grid. Since only the surface terms are evaluated

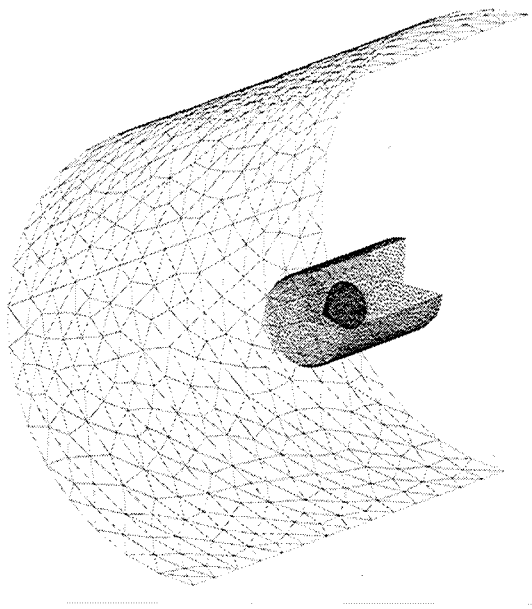

Fig. 1 Overall view of the 280,000 cell mesh.

during the acoustic prediction procedure, one does not have to take into account any phenomenon occurring outside the integration surface. The surface can also cross regions dominated by nonlinear effects.

During a run, the faces (triangles in this case) would be identified and flagged on each CPU, so that face data would be output at a prescribed sampling rate (around 50 kHz in the present case): the sampling was done in such a manner that one had at least 20 data points per wavelength, the shortest wavelength being 10 times that of the simulated shedding frequency. To avoid any redundant data, faces shared between two adjacent CPUs had to be identified at the beginning of each run, so that the number of faces whose data are output is identical to the number of triangles on the actual FW-H surface. The grid partitioning being done dynamically each time a run is initialized, the global cell indexing changes from run to run, making it necessary to run the above flagging procedure any time the program is restarted. This makes the routine independent of the number of CPUs being used. Figure 2 illustrates the regions on the surface shared between 8 processors using the Gibbs-Poole-Stockmeyer reordering algorithm.[5] As expected, each region is a neighbor to at most two other partitions, minimizing the amount of inter-processor communication.

The time step needed for a time-accurate solution is determined by the smallest cell characteristic length. This is estimated to be one third of the cell volume divided by the maximum face area. For the grid described above, this yields a time step of 9.45E-08 second at a CFL number of 0.9. The shedding frequency found during the experimental investigation of the flow is 36 Hz, for a Strouhal number equal to 0.171.

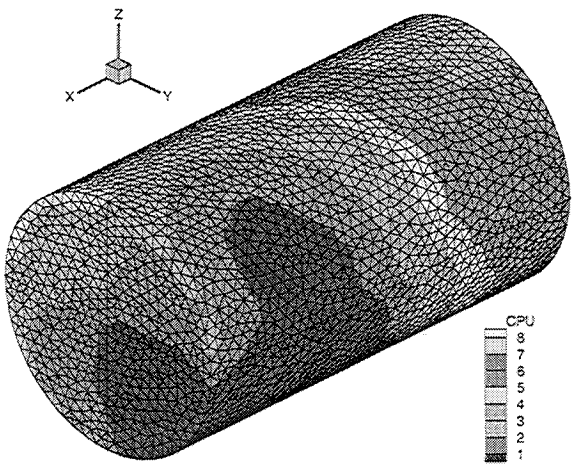

Fig. 2 Partitioning of the FW-H surface across 8 processors.

The Strouhal number was defined based on the cone diameter as $St = f_s d/U_\infty$. The numerical simulation is performed at Mach 0.2 at standard atmospheric pressure and temperature conditions, with an increased viscosity to match the experiment's Reynolds number (50,000). Scaling the Strouhal number to the simulation's Mach number yields a shedding frequency of 230 Hz. The computation of a complete shedding cycle requires roughly 46,000 iterations.

The Flow Solver - PUMA

PUMA is a computer program, written in C, for the analysis of internal and external non-reacting compressible flows over arbitrary complex geometries. PUMA uses the Message Passing Interface (MPI) to run the code in parallel. It can be run on arbitrary number of processors with very good scaling performance. Several papers[2,4] detail the benchmarking of the performance, and validation of PUMA.

PUMA is based on finite volume methods and supports mixed topology unstructured grids composed of tetrahedra, wedges, pyramids and hexahedra. The code may be run to preserve time accuracy for unsteady problems, or may be run using a pseudo-unsteady formulation to enhance the convergence to the steady state. Primitive flow quantities are computed at the cell centers. The code can be restarted from any point of time at which the solution is available from previous computations. All flow variables are stored with double precision, but may be optionally stored as single precision to save memory and communication time at the cost of reduced precision.

Parallel Machines

Computational Aeroacoustics (CAA) codes are usually very computationally intensive. Even with very powerful machines, such jobs may require days, or even months to give results. Parallel computing using Beowulf clusters offers an inexpensive way to handle such time-consuming simulations in reasonable amount of time.

Three facilities offering parallel computational power at Penn State were used for the computations - COst effective COmputing Array (COCOA),[2] COCOA2 and LionX.[6] COCOA is a Beowulf cluster comprising of 25 machines each having dual 400 MHz Pentium II processor. This facility was assembled by the authors and their colleagues in the Department of Aerospace Engineering at Penn State. The machines are connected via fast-Ethernet network which can support up to 100 Mbps bandwidth. A single Baynetworks 24-port fast-Ethernet switch with a backplane bandwidth of 2.5 Gbps is used for the networking. All the processors are dedicated to run parallel jobs. The operating system is Red Hat Linux. Message Passing Interface (MPI) is used for parallel programming and the Gnu C compiler is used for compiling PUMA. Details regarding setting up and benchmarking of COCOA may be obtained from Modi and Long[2] and COCOA's website.[7]

COCOA was primarily set up to make parallel computing facility readily available to the CFD group of the Aerospace Engineering Department at Pennsylvania State University. The total cost of the cluster was just $80,000 in the year 1998, when it was set up. Since then this facility has been intensively used for various CFD simulations. COCOA2 is a newly assembled Beowulf cluster at Penn State. It has 21 nodes each having dual 800 MHz Pentium III processors and 1 GB RAM each. The cluster has dual fast-Ethernet per node and all the nodes are connected using two HP2524 switches with channel bonding.

Figure 4 plots the parallel speedup for COCOA and COCOA2 (1 Mflop = one million floating point operations per second). Fairly good performance is obtained considering the small size of the problem. Figure 4 shows the reduction in the flop rate per processor as the grid points are distributed over a larger number of processors. This trend is typical of Beowulf clusters as the ratio of computation over communication decreases.

LionX is also a Beowulf cluster with 32 machines (each having dual 400 MHz Intel Xeon processors). These machines are connected via Myricom Myrinet with wire speed 1.28 Gbps. LionX also uses Linux with MPI for parallel programming. Performance comparison and benchmarking results for LionX can be obtained from its website.[6]

CFD Results

After initializing all variables to the freestream values, local time stepping is used to accelerate the convergence towards a physically realistic flow. This is

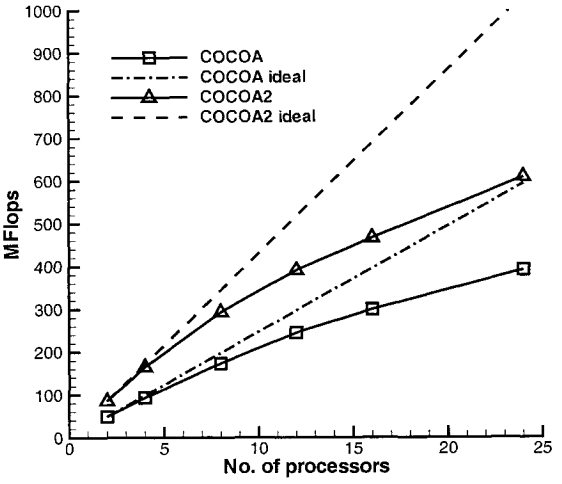

Fig. 3 Parallel speed up for COCOA and COCOA2

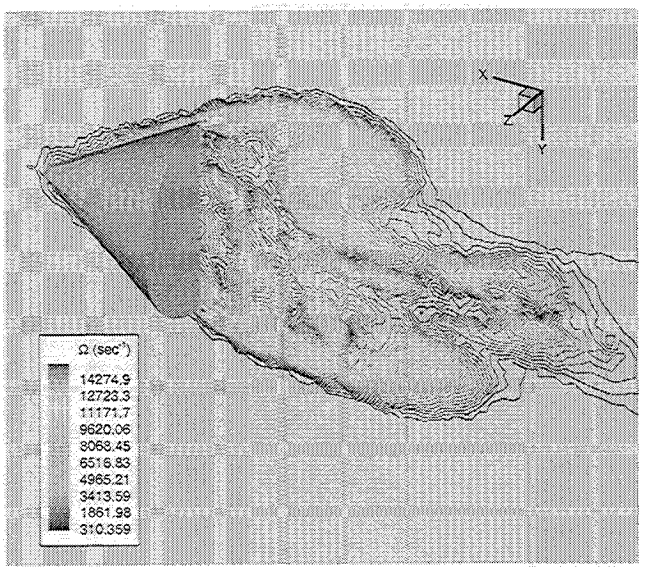

Fig. 5 Instantaneous vorticity contours.

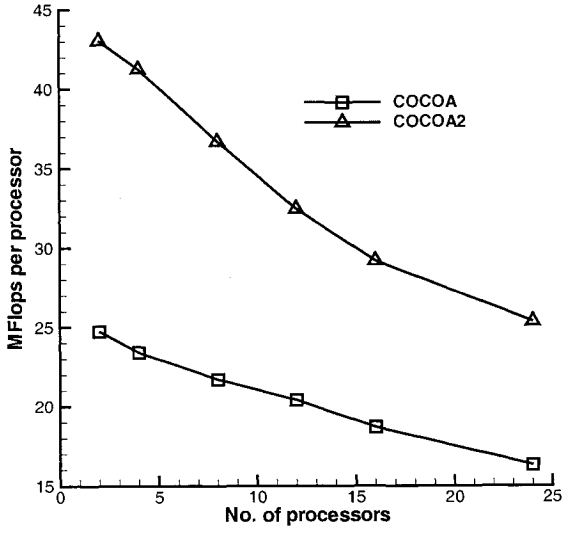

Fig. 4

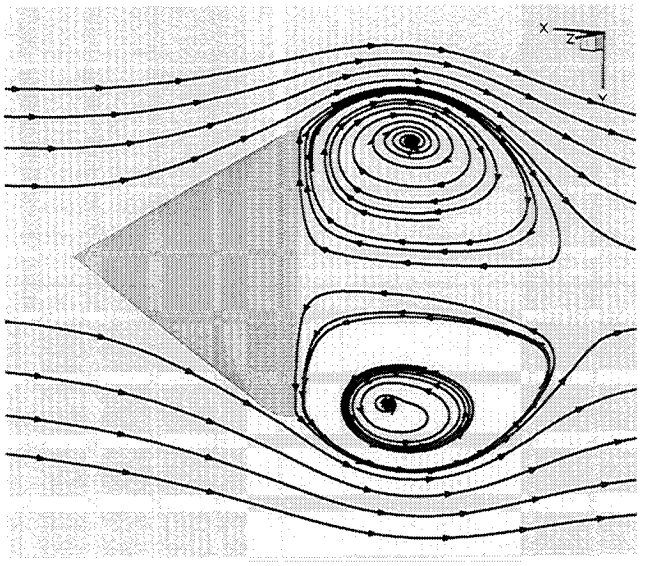

Fig. 6 Average streamlines over one shedding cycle.

done by assigning to each cell the maximum allowable time step for a given CFL number based on each cell characteristic cell length. Global time stepping is then turned on for several cycles before data are sampled, to ensure that the data on the FW-H surface follow the equations of motion. Figure 5 illustrates the vorticity patterns in the wake of the cone, showing strong recirculation phenomena. The noise from this recirculation is predicted by the FW-H module. Figure 6 is the averaged streamline contour over one shedding period, illustrating the axisymmetric bubble that was observed during Calvert's experimental study.[8]

In order to validate the solution, multiple comparisons were made between the simulation and the experimental measurements. A basic Smagorinksy sub-grid scale turbulence model[9] was added to the flow solver in order to improve the predictions, since a large-eddy simulation should yield better turbulent quantities.

Figure 7 shows the averaged streamwise velocity profiles computed by the original flow solver and those computed by the same solver combined with an LES. In all three cases the magnitude of the reverse flow velocity is under predicted when compared with experimental measurements. The predictions agree fairly well with Calvert's data in terms of the length of the recirculation zone. Past the stagnation point, the results including LES modeling follow the experimental curve more closely than those computed without any turbulence model.

Figure 8 illustrates the variation of the pressure coefficient C_p along the wake centerline. In this case, the LES having the largest sub-grid scale constant C_s greatly over-corrects the pressure drop in the near wake of the cone. The LES using a Smagorinsky constant of 0.10 matches the measured pressure data

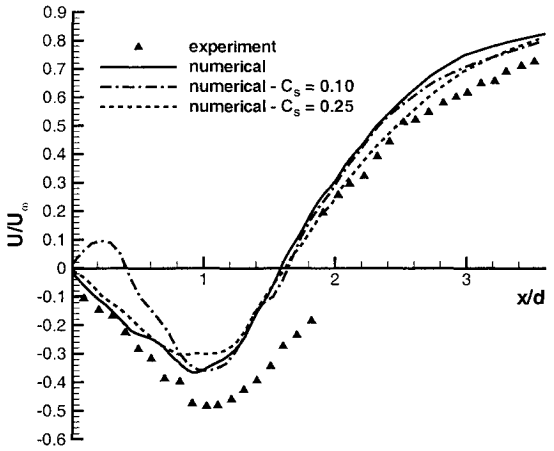

Fig. 7 Comparison of the averaged streamwise velocity with experiments for the flow solver with and without LES.

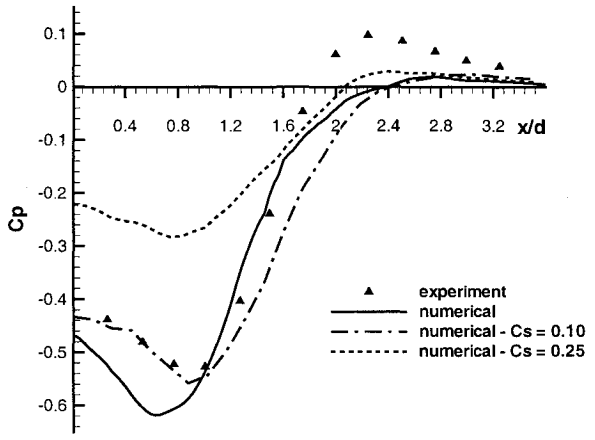

Fig. 8 Comparison of the Cp coefficient with experiment for the flow solver with and without LES.

very well until the stagnation point is reached. These results are consistent with those found in other related investigations, using either the k-ϵ turbulence model[10] or the k-ϵ-v^2 model.[11] These simulations were compared against a set of experiments[12] at a lower Reynolds number (42,000). Madabhushi[13] also used an LES with as many as 850,000 mesh points, but completely over-predicted the length of the recirculation zone.

Figure 9 shows that the averaged streamwise perturbation velocity is not well predicted using any of the sub-grid scale constants. With the grid coarsening in the far wake, the fluctuating velocities are damped very rapidly as one goes away from the cone base. It is the flow solver without any turbulence model that

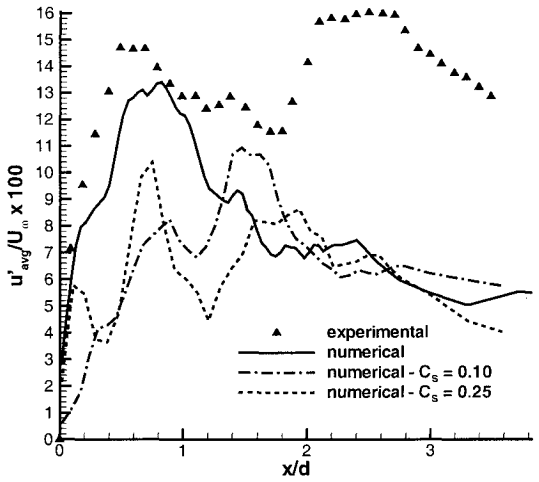

Fig. 9 Comparison of averaged streamwise perturbation velocity with experiments with and without LES.

yields unsteady velocity values that are closest to the experimental data. The solution without LES was selected to try to predict the far-field noise. It also leads to the conclusion that a more advanced turbulence model (dynamic LES, Detached Eddy Simulation) is needed to simulate such separated flows, as found in Strelets.[14]

Far-Field Noise Prediction

The two commonly used methods for far-field aerodynamic noise predictions use the Kirchhoff equation or the Ffowcs Williams-Hawkings (FW-H) equation. While the governing equation in the 'moving surface' Kirchhoff formulation[15] is a convective wave equation, the FW-H equation is an exact rearrangement of the continuity and the momentum equations into the form of an inhomogeneous wave equation. Therein lies the strength of the FW-H equation over the Kirchhoff formulation. The FW-H equation gives accurate results even if the surface of integration lies in the nonlinear flow region. This is typically the case in jets and wakes when the nonlinear region extends to large distances downstream.

In the Kirchhoff formulation the source terms are assumed to be distributed over a fictitious surface in the flow. The nonlinear effects (nonlinear wave propagation and steepening; variations in the local sound speed; and noise generated by shocks, vorticity, and turbulence in the flow field) happening within the Kirchhoff surface are captured by the surface integration terms, but the Kirchhoff formulation requires the integration surface to be placed in a linear flow region (i.e. far away from the body). This is difficult to achieve as most computational grids are generated with the concern of minimizing computations. Usually, a fine quality mesh is used near the body with increas-

ing cell size towards the outer boundaries. Therefore, the quality of the solution available in the linear flow region is generally bad. The FW-H equation, on the other hand, works fine even if the integration surface is in the nonlinear flow region. A detailed comparison of the Kirchhoff and FW-H formulations is provided in Brentner and Farassat.[16]

The solution of the full FW-H equation requires the evaluation of two surface integrals and one volume integral. The surface integrations correspond to the "thickness" noise (monopole) and the "loading" noise (dipole). The volume integration corresponds to the quadrupole term which accounts for the nonlinearity in the flow.[15,17] Evaluating the volume integral can be extremely computationally intensive and difficult to implement. Fortunately, the quadrupole term can be safely ignored for most subsonic flows as is the case in the present study.

Only recently has the FW-H equation been used on a fictitious (i.e. not the same as the body) permeable integration surface[18] - exactly like the Kirchhoff approach. di Francescantonio[18] demonstrated that when the FW-H approach is applied on a Kirchhoff-type surface, the quadrupole sources enclosed within the surface are accounted for by the surface sources. It should be noted that the "thickness" noise and the "loading" noise as obtained from solving FW-H equation do not have any physical significance if the surface of integration is chosen to be permeable (fictitious). However, when the integration surface coincides with the body, these terms provide a physical insight into the source of sound generation.

The FW-H equation is written in the standard differential form as

$$\begin{aligned} \Box^2 p'(\mathbf{x},t) &= \frac{\partial^2}{\partial x_i \partial x_j}\left[T_{ij}H(f)\right] \\ &- \frac{\partial}{\partial x_i}\left[L_i\delta(f)\right] + \frac{\partial}{\partial t}\left[(\rho_o U_n)\delta(f)\right] \end{aligned} \quad (1)$$

where L_i and U_n are defined as

$$\begin{aligned} U_n = U_i\hat{n}_i \;::\; U_i &= (1-\frac{\rho}{\rho_o})v_i + \frac{\rho u_i}{\rho_o} \\ L_i &= P_{ij}\hat{n}_j + \rho u_i(u_n - v_n) \end{aligned} \quad (2)$$

and T_{ij} is the Lighthill stress tensor. The FW-H equation can be solved using the formulation in Brentner and Farassat,[16] and the solution can be written in an integral form as

$$\begin{aligned} 4\pi p'(\mathbf{x},t) &= \int_{f=0}\left[\frac{\rho_0(\dot{U}_n + U_{\dot{n}}) + \dot{L}_r/c}{r(1-M_r)^2}\right]_{ret} \mathrm{d}S \\ &+ \int_{f=0}\left[\frac{(\rho_0 U_n + Lr/c)(r\dot{M}_r + c(M_r - M^2))}{r^2(1-M_r^3)}\right]_{ret} \mathrm{d}S \\ &+ \int_{f=0}\left[\frac{L_r - L_M}{r^2(1-M_r)^2}\right]_{ret} \mathrm{d}S \end{aligned} \quad (3)$$

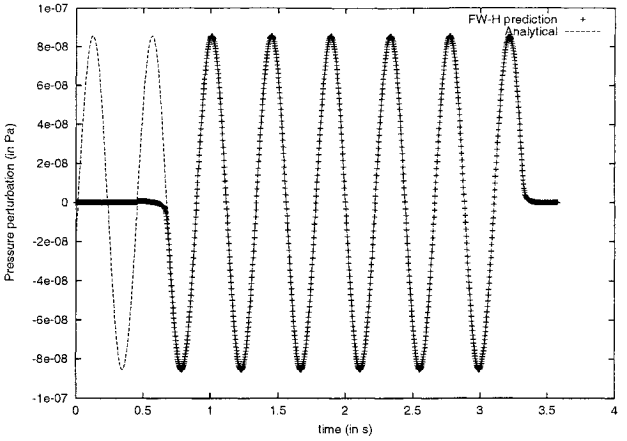

Fig. 10 Validation of the FW-H code against the analytical solution for a stationary monopole in a uniform mean flow.

The quadrupole term is ignored in the present formulation. The integrations are performed on the FW-H surface at retarded time. Since the FW-H surface is fixed relative to the body (the cone) for this study, and the flow Mach number is constant, the following terms in the above integrals are zero : $U_{\dot{n}} = \dot{M}_r = 0$. The standard time binning technique discussed by Özyörük and Long[19] is used for obtaining pressure at the observer locations.

The FW-H code and its Validation

The FW-H code is written in Fortran 90. The code was tested for a model problem - a stationary monopole in a uniform mean flow. The FW-H surface is chosen to be a box made up of rectangular panels. The analytical solution to the model problem is evaluated at the center of each panel to obtain the time history of the primitive variables on the FW-H surface. The prediction from the FW-H code (using the analytical data on the surface as input) is then compared with the analytical pressure perturbation at a point outside the surface. Figure 10 compares at an arbitrary point (300 m, 0, 0) the pressure perturbation predicted by the FW-H code and that obtained analytically for a stationary monopole source with an amplitude of 0.01 Pascals and a frequency of 2.267 Hz placed in a uniform mean flow of 0.3 Mach number. The analytical solution to this problem is :

$$\begin{aligned} \phi(\mathbf{x},t) &= \frac{\epsilon\,\exp(i\omega\tau_*)}{4\pi\left[(x+\mathrm{U}_0(\tau_*-t))^2+y^2+z^2\right]^{1/2}} \\ &\times \frac{1}{1+\frac{\mathrm{M}_0(x+\mathrm{U}_0(\tau_*-t))}{[(x+\mathrm{U}_0(\tau_*-t))^2+y^2+z^2]^{1/2}}} \end{aligned} \quad (4)$$

where τ_* is given by

$$\tau_* = t + \frac{\mathrm{M}_0 x - \left[(x^2+(1-\mathrm{M}_0{}^2)(y^2+z^2)\right]}{c(1-\mathrm{M}_0{}^2)} \quad (5)$$

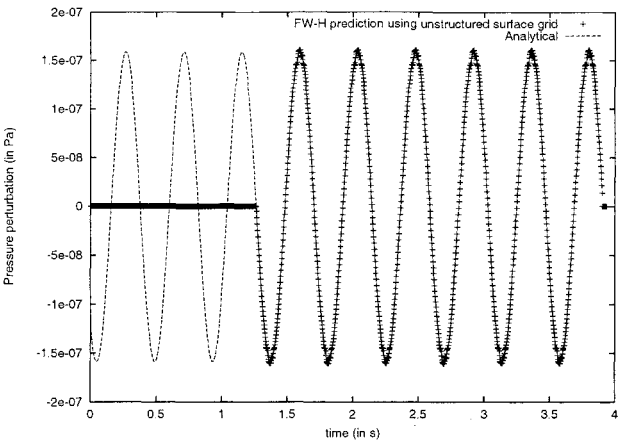

Fig. 11 Comparison of the FW-H prediction using unstructured surface grid against the analytical solution.

The unstructured grid over the cone is created such that there is an unstructured cylindrical surface enclosed in the computational domain (Fig. 1). This surface is chosen to be the permeable FW-H surface. The elements of the surface are faces of the tetrahedra, and therefore, triangles. Since these triangles are chosen from the unstructured mesh, the area and normal varies from element to element. This, however, is not a problem because the FW-H equation only requires information on a closed surface; it does not depend on the structure of the elements constituting the surface. Clustering of the surface elements is desired to increase the resolution of the sources. The FW-H surface used for the present computation is the inner cylinder in Fig. 1. This grid was used with the model problem of stationary monopole in a uniform mean flow to test if the unstructured grid poses any problems. A perfect match is observed between the FW-H prediction and the analytical solution (Fig. 11). The comparison is made at an aribtrary point (300 m, 0, 0). This confirms that an unstructured-mesh surface can be used as a FW-H surface without any loss of accuracy. Note that the first few seconds where the FW-H prediction does not match the analytical solution is the time it takes for the sound to reach the observer. This delay is more in Fig. 11 than in Fig. 10 because the unstructured FW-H surface is very small and hence, farther away from the observer point than the structured surface used for Fig. 10.

Results for the Cone

PUMA is used to obtain time accurate data (the primitive flow variables) on the FW-H surface. One complete shedding cycle of the simulation is used for far-field noise prediction. Pressure at a few points outside the FW-H surface (in the near field) is collected to compare with the predictions of the FW-H code. Four points distributed in the azimuthal direction near the base of the cone and very close to but outside the FW-H surface were chosen for comparison. The coordinates of the points are tabulated in Table 1. The cone has a base diameter of 0.02 m and a vertex angle of 60°. The center of the base of the cone is at the origin and the vertex points upstream (positive x). The FW-H surface is a cylinder of radius 0.05 m and length 0.175 m, centered at the origin.

Point No.	x (m)	y (m)	z (m)
1	0	-0.055	0
2	-0.025	0.055	0
3	0	0	0.05
4	0	0	-0.055

Table 1 Coordinates of the observer locations for comparing FW-H predictions against PUMA.

Figure 12 compares the pressure fluctuations at the four points listed in Table 1. Note that the PUMA pressure predictions have been shifted up by 20 Pascals. This is relatively a very small amount, about 0.02% of the mean pressure. We believe that this under-prediction by PUMA may be due to the dissipation caused by inadequate clustering of grid cells. It may also be due to the small sample size, and we plan to do ensemble averaging. Note that this error is of the order of magnitude of pressure pertubations predicted by the FW-H code at any point inside the FW-H surface, which should actually be zero. However, the prediction by the FW-H code agrees very well qualitatively with the PUMA solution.

Sound Directivity

The directivity of the noise from the cone was obtained by calculating the root mean squared (r.m.s.) pressure perturbation for one shedding cycle at different observer locations in azimuthal and longitudinal directions. Since the calculation for one observer location is completely independent of any other location, it is a perfect problem to run in parallel. Long and Brentner[20] suggested some self-scheduling parallel methods for multiple serial codes. However, no parallalization was done for the noise prediction results presented here.

Figure 13 plots the directivity pattern in the azimuthal direction on the plane $x = -0.1$ m, which is right behind the base of the cone. The pattern in Fig. 13 is symmetric because of the symmetry of the cone about its axis. Since the FW-H equation cannot predict the pressure fluctuation inside the FW-H surface, we can compute the noise only outside the FW-H surface. Therefore, the directivity patterns are plotted in an annular region outside the FW-H surface.

Figure 14 plots the directivity pattern in the longitudinal direction on the $z = 0$ plane. Since the noise is caused by both turbulence and fluctuating surface forces, the directivity shows several lobes.

A conventional polar directivity pattern in the longitudinal direction ($z = 0$ plane) is plotted in Fig. 15

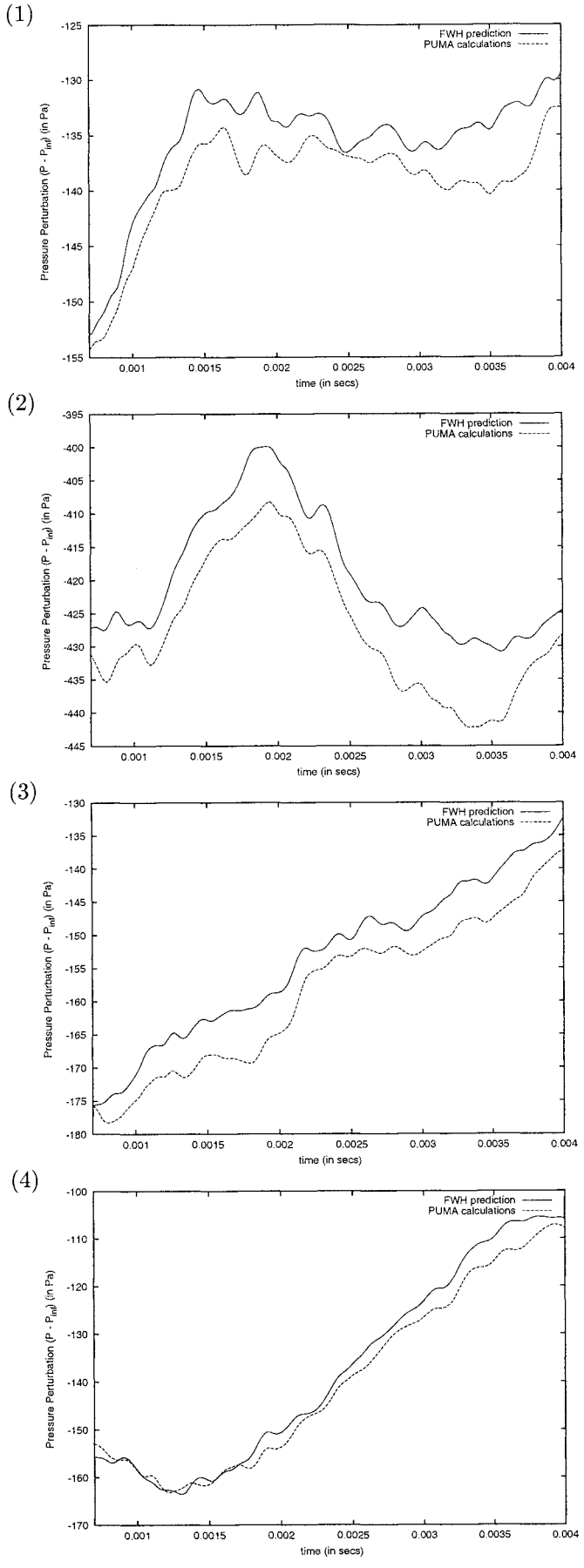

Fig. 12 Comparison of pressure fluctuation, $p - p_\infty$ as predicted by PUMA and FW-H code at various locations listed in Table 1.

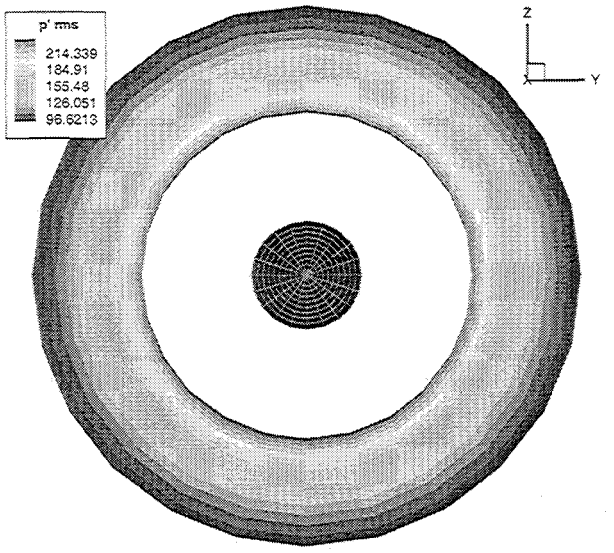

Fig. 13 Directivity of the noise in the azimuthal direction behind the base of the cone ($x = -0.1$).

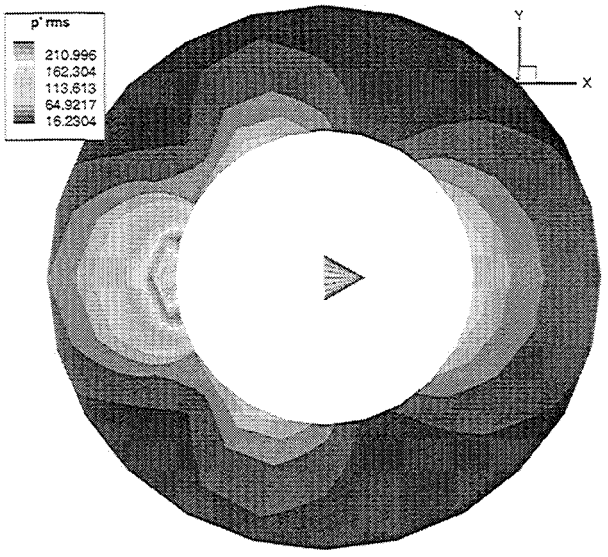

Fig. 14 Directivity of the noise in the longitudinal direction in the plane $z = 0$.

for observers at 10 different radial locations ($r = 0.15$ - 0.24 m). In Fig. 15, the cone is pointing to the right; the radial distance from the origin is equal to the r.m.s. pressure and the angle (theta) illustrates the location of the observer point in the domain.

Conclusions

Aerodynamic noise from a cone has been studied as a model problem to test the possibility of using unstructured grids for noise prediction from complicated bodies like landing gears, slats etc. A finite volume flow solver, PUMA has been used to obtain time-accurate flow data on a permeable FW-H surface. The FW-H code was validated against a model problem of a monopole in a uniform mean flow. The predictions from the FW-H code have been compared

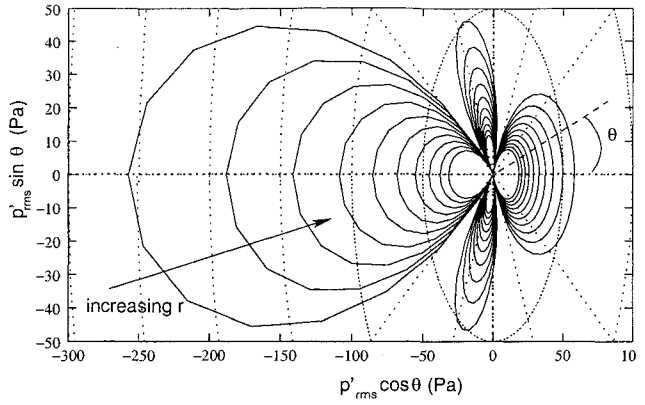

Fig. 15 Polar plot of sound directivity in $z = 0$ plane at a few radial locations.

at four observer locations in the near field with direct calculations from PUMA. Noise predictions are made for a period of one shedding cycle. The comparison is fairly accurate with only a small D.C shift error. The directivity patterns of the noise from the cone are plotted in azimuthal and longitudinal directions. The sound directivity pattern has been shown to be fairly complicated due to the complex physics inside the FW-H surface.

References

[1]Bruner, C. W. S. and Walters, R. W., "Parallelization of the Euler Equations on Unstructured Grids," AIAA Paper 1997-1894, 35th Aerospace Sciences Meeting, Jan. 1997.

[2]Modi, A. and Long, L. N., "Unsteady Separated Flow Simulations using a Cluster of Workstations," Paper 2000-0272, 38^{th} Aerospace Sciences Meeting & Exhibit, Jan. 2000.

[3]Sharma, A. and Long, L. N., "Airwake Simulations on LPD 17 Ship," Paper 2001-2589, 31^{st} AIAA Fluid Dynamics Conference and Exhibit, Anaheim, California, 2001.

[4]Modi, A., *Unsteady Separated Flow Simulations using a Cluster of Workstations*, M.S. dissertation, The Pennsylvania State University, Department of Aerospace Engineering, May 1999.

[5]I. S. Duff, A. M. E. and Reid, J. K., *Direct Methods for Sparse Matrices*, Oxford University Press, 1986.

[6]http://cac.psu.edu/beatnic/Cluster/Lionx/perf.

[7]http://cocoa.ihpca.psu.edu.

[8]Calvert, J. R., "Experiments on the Low-Speed Flow Past Cones," *Journal of Fluid Mechanics*, Vol. 27, 1967, pp. 73–289.

[9]Smagorinsky, J., "General Circulation Experiments with the Primitive Equations," *Monthly Weather Review*, Vol. 91, 1963, pp. 99–165.

[10]S. H. Johansson, L. D. and Olsson, E., "Numerical Simulation of Vortex Shedding Past Triangular Cylinders at High Reynolds Number Using a k-ϵ Turbulence Model," *International Journal For Numerical Methods in Fluids*, Vol. 16, 1993, pp. 859–878.

[11]Durbin, P. A., "Separated Flow Computations with the k-ϵ-v^2 Model," *AIAA Journal*, Vol. 33, No. 4, 1995, pp. 659–670.

[12]A. Sjunnesson, C. N. and Max, E., "LDA Measurements of Velocities and Turbulence in a Bluff Body Stabilized Flame," *Laser Anemomatry*, Vol. 3, 1991, pp. 83–90.

[13]R. K. Madabhushi, D. C. and Barber, T. J., "Unsteady Simulations of Turbulent Flow Behind a Triangular Bluff Body," paper 97-3182, $33^{r}d$ AIAA Joint Propulsion Conference and Exhibit, Seattle, WA, 1997.

[14]Strelets, M., "Detached Eddy Simulation of Massively Separated Flows," AIAA Paper 2002-0879, AIAA Aerospace Sciences Meeting and Exhibit, Reno, NV, 2001.

[15]Farassat, F. and Myers, M. K., "An Anaysis of the Quadrupole Noise Source in High Speed Rotating Blades," *Computational Acoustics - Scattering, Gaussian Beams, and Aeroacoustics*, Vol. 2, 1990, pp. 227–240.

[16]Brentner, K. S. and Farassat, F., "An Analytical Comparison of the Acoustic Analogy and Kirchoff Formulation for Moving Surfaces," *AIAA Journal*, Vol. 36, No. 8, Aug. 1998, pp. 1379–1386.

[17]Farassat, F., "Quadrupole Source in Prediction of Noise of Rotating Blades-A New Source Description," AIAA Paper 1987-2675, 1987.

[18]di Francescantonio, P., "A New Boundary Integral Formulation for the Prediction of Sound Radiation," *Journal of Sound and Vibration*, Vol. 202, No. 4, 1997, pp. 491–509.

[19]Özyörük, Y. and Long, L. N., "A New Efficient Algorithm for Computational Aeroacoustics on Parallel Procesors," *Journal of Computational Physics*, Vol. 125, 1996, pp. 135–149.

[20]Long, L. N. and Brentner, K. S., "Self-Scheduling Parallel Methods for Multiple Serial Codes with Application to WOPWOP," AIAA Paper 2000-0346, 38^{th} Aerospace Sciences Meeting & Exhibit, Reno, NV, 2000.